Extremum-seeking control for harmonic mitigation in electrical grids of marine vessels

Mark Haring, Espen Skjong, Tor Arne Johansen, *Senior Member, IEEE*, and Marta Molinas, *Member, IEEE*

***Abstract*—This work focuses on the minimization of the harmonic distortion in multi-bus electrical grids of marine vessels using a single active power filter. An active power filter is commonly used for local harmonic mitigation. However, local filtering may lead to a "whack-a-mole" effect, where the reduction of harmonic distortion at the point of installation is coupled to an increase of distortion in other grid nodes. The few existing filtering methods that consider system-wide mitigation are based on an accurate model of the power grid, which may not be available if the complexity and the scale of the grid are large. In this work, we investigate the use of an extremum-seeking control method to optimize the injection current of an active power filter for system-wide harmonic mitigation. Because the extremum-seeking control method is model free, it can be used without knowledge of the electrical grid. Moreover, the method can be implemented on top of existing approaches to combine the fast transient response of conventional harmonic-mitigation methods with the optimizing capabilities of extremum-seeking control.**

***Index Terms*—Active power filter, Extremum-seeking control, Harmonic mitigation, Power grids**

I. Introduction

EXTREMUM-SEEKING control is an adaptive-control methodology that optimizes the performance of dynamical plants based on measurements by automated tuning of plant parameters [1], [2]. The main advantage of extremum-seeking control compared to many other optimization techniques is that often no plant model is required. This makes extremum-seeking control suitable to optimize the performance of systems for which an accurate model is not available or costly to obtain. In this work, we apply extremum-seeking control to compute the injection current of an active power filter that minimizes the harmonic distortion in an electrical grid on board of a marine vessel.

Manuscript received June 21, 2017; revised February 16, 2018; accepted April 2, 2018. This work is sponsored by the Research Council of Norway and Ulstein Power & Control AS, project number 241205, by the KMB project D2V, project number 210670, and through the Centres of Excellence funding scheme, project number 223254 - NTNU AMOS.

M. Haring and T. A. Johansen are with the Centre for Autonomous Marine Operations and Systems, Department of Engineering Cybernetics, NTNU, Norwegian University of Science and Technology, 7491 Trondheim, Norway (phone: +47 73590671; fax: +47 73594599; e-mail: mark.haring@ntnu.no, tor.arne.johansen@ntnu.no).

E. Skjong is with Ulstein Blue Ctrl AS, 6018 Ålesund, Norway (e-mail: espen.skjong@ulstein.com).

M. Molinas is with the Department of Engineering Cybernetics, NTNU, Norwegian University of Science and Technology, 7491 Trondheim, Norway (e-mail: marta.molinas@ntnu.no).

There are many challenges related to the power quality on board of marine vessels; see for example [3], [4]. One of these challenges is harmonic distortion. Harmonic distortion in alternating-current power grids is the presence of harmonic components in current and voltage signals other than the fundamental frequency. Harmonic distortion is caused by nonlinear loads in the power grid. Although low levels of harmonic distortion are often tolerated, high levels of harmonic distortion can result in significant power losses and an increased wear of mechanical components in the grid. Severe harmonic distortion may even lead to overheating and failure of components. Several harmonic mitigation methods such as passive filtering, active filtering and phase multiplication are discussed in [5]–[7]. In practice, often a combination of mitigation devices is employed to enhance power quality.

An active power filter injects a current to counteract the harmonic distortion generated by the nonlinear loads in the power grid. The control of active power filters for local filtering has been studied extensively in [7]–[10] and references therein. Although local filtering decreases the harmonic distortion at the point of installation, it may simultaneously increase the distortion in other buses of the grid, leading to a "whack-a-mole" effect [11]. There are several methods that avoid the whack-a-mole using a system-wide approach. To avoid the whack-a-mole, the harmonic distortion in multi-bus electrical grids may be mitigated by connecting an active power filter to each grid node. However, this is often not a viable solution for marine vessels due to the large economic cost and the limited available space on board the vessel.

Contrary to local filtering, there are methods that apply a system-wide approach using a limited number of active power filters (often only a single active power filter is used) to avoid whack-a-mole issues. These methods are based on computing the relation between the current injections of the active power filters and the corresponding harmonic distortion in the grid nodes with the help of a grid model. To find the optimal current injection of an active power filter for system-wide mitigation under static load conditions, a cost function is introduced in [12], [13] to weigh the harmonic voltage distortion in the buses of the grid. The impedance matrix of the power grid is used to link the voltage distortion to the current injection of each active power filter. The optimal current injection is subsequently obtained by minimizing the cost function. In [14]–[18], a model-predictive control method is presented for system-wide harmonic mitigation. The methods in [12], [13] and in [14]–[18] have two major drawbacks that limit

their applicability. First, an accurate grid model is required to effectively mitigate the harmonic distortion in the electric grid. Obtaining an accurate grid model may require modeling of many components in the grid as well as their interconnections. Hence, the effort and expenses of applying these methods may be substantial, especially if the complexity and the scale of the grid are large. Second, the underlying optimization problems on which these methods are based need to be solved at every sampling instance if the methods are to be implemented in real time. Depending on the scale and complexity of the grid, one may have to settle for a relatively coarse grid model to avoid that the computational effort exceeds the available computational capacity to solve the optimization problem in the limited available time. In turn, a coarse grid model may impair the performance of the methods.

The contributions of this work can be summarized as follows. First, we present a discrete-time extremum-seeking control method to optimize the injection current of a single active power filter for system-wide harmonic mitigation in electric grids of marine vessels. We note that the presented method can easily be extended to include several active power filters using a multivariable extremum-seeking control approach similar to [19], [20]. The main advantage of the presented extremum-seeking method is that it does not require a model of the grid. Contrary to alternative model-based methods, it is computationally cheap and easily scalable to a grid with an arbitrary number of nodes. Second, the extremum-seeking controller can be implemented on top of local active filtering approaches to combine the fast transient response of conventional harmonic-mitigation methods with the system-wide optimizing capabilities of extremum-seeking control.

The organization of this work is as follows. We formulate the harmonic-mitigation problem in Section II. The extremum-seeking control method is introduced in Section III. A case study of a diesel-electric ship with a three-bus electrical grid with distributed generators is presented in Section IV. The conclusion of this work is given in Section V.

We introduce the following notations. $\mathbf{I}$ is the identity matrix. $\mathbf{0}$ is the zero matrix. $\mathbf{M}^T$ denotes the transpose of the matrix $\mathbf{M}$.

II. Harmonic-mitigation problem formulation

Consider a stable balanced three-phase three-wire multi-bus power grid. An active power filter is connected to one of the buses of the grid. Suppose we want to use the active power filter to minimize the harmonic distortion in n buses of the electrical grid. Let these buses be numbered one to n. Moreover, let the three phases be denoted by a, b and c. For constant loads and steady-state conditions, a simplified representation of the voltages in bus j for the phases a, b and c is given by

$$\begin{aligned} V_{j,a}(t) &= \sum_{h=1}^{\infty} A_j^h \sin\left(\frac{2\pi h t}{T_f} + \phi_j^h\right), \\ V_{j,b}(t) &= \sum_{h=1}^{\infty} A_j^h \sin\left(\frac{2\pi h t}{T_f} - \frac{2\pi}{3}h + \phi_j^h\right), \\ V_{j,c}(t) &= \sum_{h=1}^{\infty} A_j^h \sin\left(\frac{2\pi h t}{T_f} + \frac{2\pi}{3}h + \phi_j^h\right), \end{aligned} \tag{1}$$

for $j = \{1, 2, \ldots, n\}$, where A_j^h and ϕ_j^h are the amplitude and the phase offset of the hth-order harmonic of the voltages in bus j, where t denotes the time, and where T_f is the period of the fundamental frequency. We note that the voltage contributions for interharmonic frequencies may be substantial in some marine applications [21]. However, these are neglected here in order to focus on the harmonic mitigation problem. To balance the objective of minimizing the harmonic distortion in the n buses, we introduce the following cost function consisting of the sum of squared voltage amplitudes of the dominant distortion harmonics in the electrical grid, similar to [12], [13]:

$$J(A_1^{h_1}, A_2^{h_1}, \ldots, A_n^{h_m}) = \sum_{j=1}^{n} \sum_{h \in \mathcal{H}} \beta_j^h \left(A_j^h\right)^2, \tag{2}$$

where β_j^h is a chosen positive weighting constant for the voltage amplitude A_j^h, and where $\mathcal{H} = \{h_1, h_2, \ldots, h_m\}$ is a set consisting of the orders of m dominant harmonics in the electrical grid to be mitigated, where each element of $\mathcal{H}$ is unique and larger than one. As pointed out in [13], the cost function in (2) is suited to incorporate several harmonic-distortion measures, including the total harmonic distortion, the telephone influence factor and the motor-load loss function.

To minimize the harmonic distortion in the buses, we provide the following current reference to the active power filter for the three phases a, b and c:

$$\begin{aligned} i_{r,a}(t) &= \sum_{h \in \mathcal{H}} i_{r,a}^h(t), \quad i_{r,b}(t) = \sum_{h \in \mathcal{H}} i_{r,b}^h(t), \\ i_{r,c}(t) &= \sum_{h \in \mathcal{H}} i_{r,c}^h(t), \end{aligned} \tag{3}$$

with

$$\begin{aligned} i_{r,a}^h(t) &= u_1^h \sin\left(\frac{2\pi h t}{T_f}\right) + u_2^h \cos\left(\frac{2\pi h t}{T_f}\right), \\ i_{r,b}^h(t) &= u_1^h \sin\left(\frac{2\pi h t}{T_f} - \frac{2\pi}{3}h\right) + u_2^h \cos\left(\frac{2\pi h t}{T_f} - \frac{2\pi}{3}h\right), \\ i_{r,c}^h(t) &= u_1^h \sin\left(\frac{2\pi h t}{T_f} + \frac{2\pi}{3}h\right) + u_2^h \cos\left(\frac{2\pi h t}{T_f} + \frac{2\pi}{3}h\right) \end{aligned} \tag{4}$$

and parameters $u_1^{h_1}, u_2^{h_1}, \ldots, u_2^{h_m}$. By feeding the references in (3) to the active power filter, the active power filter generates a current injection for the three phases with feedback from the power grid. Assuming that the generated current injection is equal to the reference current and that the bus connections in the grid can be modeled by linear impedance, the impedance matrix of the grid can be used to determine the effect of the current reference on the voltages in the buses; see [12], [13].

For example, the voltage difference in bus j for phase a due to the current injection of the active filter can be written as

$$\Delta V_{j,a}(t) = \sum_{h\in\mathcal{H}} \left(\left(Z^h_{R,j}u^h_1 + Z^h_{I,j}u^h_2\right)\sin\left(\frac{2\pi ht}{T_f}\right) + \left(Z^h_{R,j}u^h_2 - Z^h_{I,j}u^h_1\right)\cos\left(\frac{2\pi ht}{T_f}\right)\right) \tag{5}$$

for $j \in \{1, 2, \ldots, n\}$. Here, $Z^h_{R,j}$ and $Z^h_{I,j}$ denote the real and imaginary part of the impedance that links the hth harmonic of the current injection of the active power filter to the voltage of bus j. Similar expressions for the voltage differences for the phases b and c can be obtained by applying appropriate phase shifts as in (1) and (3). Now, let the voltage in bus j for phase a prior to the current injection be denoted by

$$V^0_{j,a}(t) = \sum_{h=1}^{\infty} A^{0,h}_j \sin\left(\frac{2\pi ht}{T_f} + \phi^{0,h}_j\right), \tag{6}$$

such that the voltage after the current injection is given by

$$V_{j,a}(t) = V^0_{j,a}(t) + \Delta V_{j,a}(t). \tag{7}$$

From (1) and (5)-(7), it follows that

$$\left(A^h_j\right)^2 = \left(A^{0,h}_j\cos(\phi^{0,h}_j) + Z^h_{R,j}u^h_1 + Z^h_{I,j}u^h_2\right)^2 + \left(A^{0,h}_j\sin(\phi^{0,h}_j) + Z^h_{R,j}u^h_2 - Z^h_{I,j}u^h_1\right)^2 \tag{8}$$

for all $j \in \{1, 2, \ldots, n\}$ and all $h \in \mathcal{H}$. By combining (8) and the cost function in (2), we obtain that the output of the cost function is a function of the parameters $u^{h_1}_1, u^{h_1}_2, \ldots, u^{h_m}_2$, that is, $J(A^{h_1}_1, A^{h_1}_2, \ldots, A^{h_m}_n) = F(\mathbf{u}^{h_1}, \mathbf{u}^{h_2}\ldots, \mathbf{u}^{h_m})$, with

$$\begin{aligned} &F(\mathbf{u}^{h_1}, \mathbf{u}^{h_2}\ldots, \mathbf{u}^{h_m}) \\ &= \sum_{j=1}^{n}\sum_{h\in\mathcal{H}} \beta^h_j \left(\left(A^{0,h}_j\cos(\phi^{0,h}_j) + Z^h_{R,j}u^h_1 + Z^h_{I,j}u^h_2\right)^2 \right. \\ &\quad \left. + \left(A^{0,h}_j\sin(\phi^{0,h}_j) + Z^h_{R,j}u^h_2 - Z^h_{I,j}u^h_1\right)^2 \right) \end{aligned} \tag{9}$$

and $\mathbf{u}^h = [u^h_1, u^h_2]^T$ for all $h \in \mathcal{H}$. We refer to the function F as the objective function. To minimize the cost function in (2), we aim to find the values of the parameters $u^{h_1}_1, u^{h_1}_2, \ldots, u^{h_m}_2$ for which the value of the objective function is minimal. To simplify the task at hand, we note that

$$F(\mathbf{u}^{h_1}, \mathbf{u}^{h_2}\ldots, \mathbf{u}^{h_m}) = \sum_{h\in\mathcal{H}} F^h(\mathbf{u}^h), \tag{10}$$

with $\mathbf{u}^h = [u^h_1, u^h_2]^T$ and

$$F^h(\mathbf{u}^h) = \sum_{j=1}^{n} \beta^h_j \left(\left(A^{0,h}_j\cos(\phi^{0,h}_j) + Z^h_{R,j}u^h_1 + Z^h_{I,j}u^h_2\right)^2 + \left(A^{0,h}_j\sin(\phi^{0,h}_j) + Z^h_{R,j}u^h_2 - Z^h_{I,j}u^h_1\right)^2 \right). \tag{11}$$

Hence, minimizing the objective function F in (9) is equivalent to minimizing each quadratic function F^h in (11). Contrary to [12], [13] and [14]–[18], we assume that detailed knowledge of the electrical grid is not available. The active power filter and the power grid are regarded as a black box; see Fig. 1. This

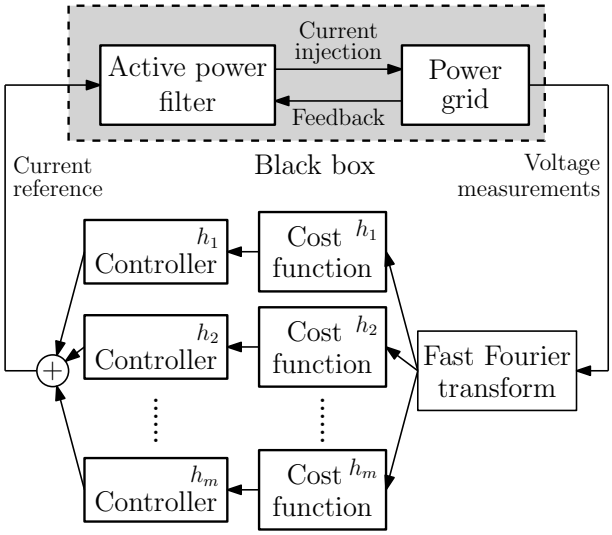

Fig. 1. Harmonic-mitigation scheme.

implies that the impedance matrix of the grid and thus the constants $Z^h_{R,j}$ and $Z^h_{I,j}$ are unknown. Hence, the functions F^h are unknown and their minima cannot be computed analytically.

To minimize the cost function in (2), we introduce m extremum-seeking controllers to find the values of the parameters u^h_1 and u^h_2 that minimize the function F^h and generate the corresponding partial current reference in (4) for each $h \in \mathcal{H}$. The current reference in (3) that minimizes the cost function in (2) is subsequently obtained by summing the partial current references produced by the controllers. In order to determine the parameters u^h_1 and u^h_2 that minimize the function F^h, each extremum-seeking controllers minimizes the cost function

$$J^h(A^h_1, A^h_2, \ldots, A^h_n) = \sum_{j=1}^{n} \beta^h_j \left(A^h_j\right)^2 \tag{12}$$

for one harmonic $h \in \mathcal{H}$, where the voltage amplitudes $A^h_1, A^h_2, \ldots, A^h_n$ are obtained by applying a fast Fourier transform algorithm to measurements of the voltage signals of the buses. A comparison of different algorithms to compute coefficients in Fourier series for electric power system applications is provided in [22]. We note that, similar to [12], [13] and [14]–[18], the presented harmonic-mitigation solution requires communication between the buses to process the voltage measurements. An overview of the harmonic-mitigation scheme is given in Fig. 1.

The assumptions in this section that are used to obtain the expression of the objective function in (9) may not hold in practical applications: the power grid may be unbalanced, the active power filter may generate a current injection that differs from the current reference, modeling of the bus connections by linear impedance may be inaccurate, etc. Nonetheless, the assumptions in this section often appear to be be good approximations in practice and are common in many text books about harmonic mitigation; see for example [7]. As we will see in the case study in Section IV, extremum-seeking control is a robust optimization technique that may

be successfully applied even if the assumptions in this section do not entirely hold.

III. Extremum-seeking control method

For each $h \in \mathcal{H}$, we introduce a discrete-time extremum-seeking controller to find the values of the parameters $\mathbf{u}^h = [u_1^h, u_2^h]^T$ for which the objective function F^h in (11) exhibits a minimum. Let the sampling time of the extremum-seeking controller be denoted by the positive constant T_s. At each sampling instance $t = kT_s$ (with counter $k = 0, 1, 2, ...$), the extremum-seeking controller updates the values of the parameters $\mathbf{u}^h$ and the corresponding partial current reference to the active power filter in (4). Let $\mathbf{u}_k^h = [u_{1,k}^h, u_{2,k}^h]^T$ denote the vector of parameter values at time $t = kT_s$. Moreover, let $y_k^h = J^h(A_{1,k}^h, A_{2,k}^h, \ldots, A_{n,k}^h)$, where the inputs $A_{1,k}^h, \ldots, A_{n,k}^h$ of the cost function J^h in (12) are obtained by taking the fast Fourier transform of the measured voltage signals of the buses for the time interval $(kT_s - T_f, kT_s]$. In Section II, we implicitly assumed that u_1^h and u_2^h are constant such that $J^h(A_1^h, A_2^h, \ldots, A_n^h)$ is equal to $F^h(\mathbf{u}^h)$ under steady-state conditions. For a stable power grid, as we assume here, the output y_k^h of J^h remains close to $F^h(\mathbf{u}_k^h)$ for suitable initial conditions of the active power filter and the electrical grid if $\mathbf{u}_k^h$ is sufficiently slow compared to the dynamics of the active power filter and the electrical grid. This can be formally proved using a singular-perturbation method as in [23], [24]. Due to the use of the fast Fourier transform, a distributed time delay is introduced between $\mathbf{u}_k^h$ and y_k^h. This delay is especially large if $T_f \gg T_s$. Bounded time delays in extremum-seeking schemes can be handled by making the parameter vector $\mathbf{u}_k^h$ sufficiently slowly time varying; see for example [25], [26]. In this work, however, we aim to compensate for the time delay, which may help to enable a faster convergence of the extremum-seeking controller [27], [28]. We model the relation between $\mathbf{u}_k^h$ and y_k^h as

$$y_k^h = \frac{1}{N} \sum_{r=0}^{N-1} F^h(\mathbf{u}_{k-r}^h), \tag{13}$$

where we assume that $N = \frac{T_f}{T_s}$ is a positive integer. Linear interpolation can be applied to obtain a similar expression if $\frac{T_f}{T_s}$ is not a positive integer. We note that (13) implies that $y_k^h = F^h(\mathbf{u}_k^h)$ if $\mathbf{u}_k^h$ is constant and that a similar argument as before can be invoked to prove that (13) is an accurate approximation for suitable initial conditions if $\mathbf{u}_k^h$ is sufficiently slowly time varying.

Next, we introduce a perturbation-based extremum-seeking controller. The controller steers the parameters $\mathbf{u}_k^h$ towards the point of optimal harmonic mitigation using a gradient-descent approach based on an estimate of the gradient of the objective function F^h. We define

$$\mathbf{u}_k^h = \hat{\mathbf{u}}_k^h + \alpha_{\boldsymbol{\omega}}^h \boldsymbol{\omega}_k^h, \quad \boldsymbol{\omega}_k^h = \left[\sin\left(\frac{2\pi k}{N_{\boldsymbol{\omega}}^h}\right), \cos\left(\frac{2\pi k}{N_{\boldsymbol{\omega}}^h}\right)\right]^T, \tag{14}$$

where $\boldsymbol{\omega}_k^h$ is a vector of perturbations with amplitude $\alpha_{\boldsymbol{\omega}}^h > 0$. The tuning parameter $N_{\boldsymbol{\omega}}^h > 0$ is an integer related to the frequency of the perturbations in (14). From (14) and Taylor's theorem, we have that

$$F^h(\mathbf{u}_k^h) = F^h(\hat{\mathbf{u}}_k^h) + \alpha_{\boldsymbol{\omega}}^h \frac{dF^h}{d\mathbf{u}^h}(\hat{\mathbf{u}}_k^h)\boldsymbol{\omega}_k^h + \left(\alpha_{\boldsymbol{\omega}}^h\right)^2 R_{1,k}, \tag{15}$$

where $\left(\alpha_{\boldsymbol{\omega}}^h\right)^2 R_{1,k}$ is the remainder of the Taylor series expansion. $R_{1,k}$ is a function of the uniformly bounded vector $\boldsymbol{\omega}_k^h$ in (14) and the Hessian of the quadratic function F^h in (11). Hence, it is independent of $\mathbf{u}_k^h$ and uniformly bounded, which implies that the remainder term $\left(\alpha_{\boldsymbol{\omega}}^h\right)^2 R_{1,k}$ can be made arbitrarily small by choosing sufficiently small values of $\alpha_{\boldsymbol{\omega}}^h$. Define $\Delta\hat{\mathbf{u}}_k^h = \hat{\mathbf{u}}_{k+1}^h - \hat{\mathbf{u}}_k^h$. Similar to (15), it follows from Taylor's theorem that

$$F^h(\hat{\mathbf{u}}_{k+1}^h) = F^h(\hat{\mathbf{u}}_k^h) + \alpha_{\boldsymbol{\omega}}^h \frac{dF^h}{d\mathbf{u}^h}(\hat{\mathbf{u}}_k^h)\frac{\Delta\hat{\mathbf{u}}_k^h}{\alpha_{\boldsymbol{\omega}}^h} + \left(\alpha_{\boldsymbol{\omega}}^h\right)^2 R_{2,k}, \tag{16}$$

and

$$\alpha_{\boldsymbol{\omega}}^h \frac{dF^h}{d\mathbf{u}^h}(\hat{\mathbf{u}}_{k+1}^h) = \alpha_{\boldsymbol{\omega}}^h \frac{dF^h}{d\mathbf{u}^h}(\hat{\mathbf{u}}_k^h) + \left(\alpha_{\boldsymbol{\omega}}^h\right)^2 \mathbf{R}_{3,k}^T. \tag{17}$$

Assuming that $\frac{\Delta\hat{\mathbf{u}}_k^h}{\alpha_{\boldsymbol{\omega}}^h}$ is uniformly bounded with a bound that is independent of $\alpha_{\boldsymbol{\omega}}^h$, by using similar reasoning as for $R_{1,k}$, it follows that $R_{2,k}$ and $\mathbf{R}_{3,k}$ are uniformly bounded, which implies that the remainder terms $\left(\alpha_{\boldsymbol{\omega}}^h\right)^2 R_{2,k}$ and $\left(\alpha_{\boldsymbol{\omega}}^h\right)^2 \mathbf{R}_{3,k}^T$ can be made arbitrarily small by choosing sufficiently small values of $\alpha_{\boldsymbol{\omega}}^h$. From (14)-(17), we obtain that (13) can be accurately approximated by

$$y_k^h = F^h(\hat{\mathbf{u}}_k^h) + \alpha_{\boldsymbol{\omega}}^h \frac{dF^h}{d\mathbf{u}^h}(\hat{\mathbf{u}}_k^h)\left(\frac{1}{N}\sum_{r=0}^{N-1}\frac{\mathbf{u}_{k-r}^h}{\alpha_{\boldsymbol{\omega}}^h} - \frac{\hat{\mathbf{u}}_k^h}{\alpha_{\boldsymbol{\omega}}^h}\right) \tag{18}$$

for sufficiently small values of $\alpha_{\boldsymbol{\omega}}^h$ if $\frac{\Delta\hat{\mathbf{u}}_k^h}{\alpha_{\boldsymbol{\omega}}^h}$ is uniformly bounded with a bound that is independent of $\alpha_{\boldsymbol{\omega}}^h$. Now, let us define the vector

$$\mathbf{m}_k^h = \begin{bmatrix} F^h(\hat{\mathbf{u}}_k^h) \\ \alpha_{\boldsymbol{\omega}}^h \left(\frac{dF^h}{d\mathbf{u}^h}(\hat{\mathbf{u}}_k^h)\right)^T \end{bmatrix}. \tag{19}$$

By combining (16)-(19), we obtain that the dynamic model

$$\begin{aligned} \mathbf{m}_{k+1}^h &= \mathbf{A}_k^h \mathbf{m}_k^h \\ y_k^h &= \mathbf{C}_k^h \mathbf{m}_k^h, \end{aligned} \tag{20}$$

with

$$\mathbf{A}_k^h = \begin{bmatrix} 1 & \left(\frac{\Delta\hat{\mathbf{u}}_k^h}{\alpha_{\boldsymbol{\omega}}^h}\right)^T \\ \mathbf{0} & \mathbf{I} \end{bmatrix} \tag{21}$$

and

$$\mathbf{C}_k^h = \begin{bmatrix} 1 & \left(\frac{1}{N}\sum_{r=0}^{N-1}\frac{\mathbf{u}_{k-r}^h}{\alpha_{\boldsymbol{\omega}}^h} - \frac{\hat{\mathbf{u}}_k^h}{\alpha_{\boldsymbol{\omega}}^h}\right)^T \end{bmatrix}, \tag{22}$$

is accurate if $\mathbf{u}_k^h$ is sufficiently slowly time varying, if $\frac{\Delta\hat{\mathbf{u}}_k^h}{\alpha_{\boldsymbol{\omega}}^h}$ is uniformly bounded with a bound that is independent of $\alpha_{\boldsymbol{\omega}}^h$, and if $\alpha_{\boldsymbol{\omega}}^h$ is sufficiently small. We note the vector $\mathbf{m}_k^h$ in (19) contains the gradient of the objective function F^h scaled by the tuning parameter $\alpha_{\boldsymbol{\omega}}^h$. Therefore, an estimate of the gradient of the objective function can be obtained by estimating the state vector $\mathbf{m}_k^h$ of the model. We note that the perturbations in

(14) are essential for estimating the gradient of the objective function because they ensure that the model (20) is uniformly observable under appropriate tuning conditions.

We introduce the following three-step observer [29] to estimate the state vector $\mathbf{m}_k^h$:

Step $\mathbf{1} \rightarrow \mathbf{2}$ (correction step):

$$\begin{aligned}\hat{\mathbf{m}}_{k|2}^h &= \hat{\mathbf{m}}_{k|1}^h + \mathbf{L}_{k|1}^h \left(y_k^h - \mathbf{C}_k^h \hat{\mathbf{m}}_{k|1}^h\right),\\ \mathbf{Q}_{k|2}^h &= \left(\mathbf{I} - \mathbf{L}_{k|1}^h \mathbf{C}_k^h\right) \mathbf{Q}_{k|1}^h \left(\mathbf{I} - \mathbf{L}_{k|1}^h \mathbf{C}_k^h\right)^T \\ &\quad + \frac{1}{1-\lambda_{\mathbf{m}}^h} \mathbf{L}_{k|1}^h \left(\mathbf{L}_{k|1}^h\right)^T,\end{aligned} \tag{23}$$

Step $\mathbf{2} \rightarrow \mathbf{3}$ (regularization step):

$$\begin{aligned}\hat{\mathbf{m}}_{k|3}^h &= \hat{\mathbf{m}}_{k|2}^h - \mathbf{L}_{k|2}^h \mathbf{D} \hat{\mathbf{m}}_{k|2}^h,\\ \mathbf{Q}_{k|3}^h &= \left(\mathbf{I} - \mathbf{L}_{k|2}^h \mathbf{D}\right) \mathbf{Q}_{k|2}^h \left(\mathbf{I} - \mathbf{L}_{k|2}^h \mathbf{D}\right)^T \\ &\quad + \frac{1}{\sigma_r^h (1-\lambda_{\mathbf{m}}^h)} \mathbf{L}_{k|2}^h \left(\mathbf{L}_{k|2}^h\right)^T,\end{aligned} \tag{24}$$

Step $\mathbf{3} \rightarrow \mathbf{1}$ (prediction step):

$$\begin{aligned}\hat{\mathbf{m}}_{k+1|1}^h &= \mathbf{A}_k^h \hat{\mathbf{m}}_{k|3}^h,\\ \mathbf{Q}_{k+1|1}^h &= \frac{1}{\lambda_{\mathbf{m}}^h} \mathbf{A}_k^h \mathbf{Q}_{k|3}^h \left(\mathbf{A}_k^h\right)^T,\end{aligned} \tag{25}$$

with

$$\begin{aligned}\mathbf{L}_{k|1}^h &= \mathbf{Q}_{k|1}^h \left(\mathbf{C}_k^h\right)^T \left(\frac{1}{1-\lambda_{\mathbf{m}}^h} + \mathbf{C}_k^h \mathbf{Q}_{k|1}^h \left(\mathbf{C}_k^h\right)^T\right)^{-1},\\ \mathbf{L}_{k|2}^h &= \mathbf{Q}_{k|2}^h \mathbf{D}^T \left(\frac{1}{\sigma_r^h (1-\lambda_{\mathbf{m}}^h)} \mathbf{I} + \mathbf{D} \mathbf{Q}_{k|2}^h \mathbf{D}^T\right)^{-1}\end{aligned} \tag{26}$$

and

$$\mathbf{D} = \begin{bmatrix}\mathbf{0} & \mathbf{I}\end{bmatrix}. \tag{27}$$

The observer in (23)-(25) is comparable to a Kalman filter, where $\hat{\mathbf{m}}_{k|3}^h$ is an estimate of the state vector $\mathbf{m}_k^h$, and where $\mathbf{Q}_{k|3}^h$ resembles the positive-definite state covariance matrix of the Kalman filter. The vectors $\hat{\mathbf{m}}_{k|1}^h$ and $\hat{\mathbf{m}}_{k|2}^h$ and the positive-definite matrices $\mathbf{Q}_{k|1}^h$ and $\mathbf{Q}_{k|2}^h$ are intermediate variables. The observer is initiated by selecting the values of $\hat{\mathbf{m}}_{k|1}^h$ and $\mathbf{Q}_{k|1}^h$, after which (23)-(25) can be used to obtain an estimate of the state vector for each subsequent time step. The tuning parameter $\lambda_{\mathbf{m}}^h \in (0,1)$ is sometimes referred to as the forgetting factor [30]. Its value determines the convergence speed of the observer: a value close to zero implies a fast convergence, while a value close to one implies a slow convergence. Commonly, the value of $\lambda_{\mathbf{m}}^h$ is set to be close to one. Contrary to the Kalman filter, the observer contains a regularization step that prevents the elements of the matrix $\mathbf{Q}_{k|3}^h$ from becoming excessively large if the parameter vector $\mathbf{u}_k^h$ is momentarily not sufficiently rich to accurately estimate the state vector $\mathbf{m}_k^h$. Because regularization deteriorates the estimate of the state vector $\mathbf{m}_k^h$, the regularization constant $\sigma_r^h > 0$ is commonly chosen to be small.

Noting that $\hat{\mathbf{m}}_{k|3}^h$ is an estimate of the state vector $\mathbf{m}_k^h$, we obtain that $\mathbf{D}\hat{\mathbf{m}}_{k|3}^h$ is an estimate of the gradient of the objective function F^h scaled by the tuning parameter $\alpha_{\boldsymbol{\omega}}^h$. With this in mind, we define the following gradient-descent optimizer to guide $\mathbf{u}_k^h$ towards the minimum of the objective function F^h:

$$\hat{\mathbf{u}}_{k+1}^h = \hat{\mathbf{u}}_k^h - \lambda_{\mathbf{u}}^h \frac{\eta_{\mathbf{u}}^h \mathbf{D}\hat{\mathbf{m}}_{k|3}^h}{\eta_{\mathbf{u}}^h + \lambda_{\mathbf{u}}^h \|\mathbf{D}\hat{\mathbf{m}}_{k|3}^h\|}, \tag{28}$$

with linear gain $\lambda_{\mathbf{u}}^h > 0$ and normalization gain $\eta_{\mathbf{u}}^h > 0$. The linear gain $\lambda_{\mathbf{u}}^h$ influences the convergence speed of the optimizer: a large value results in a fast convergence, while a low value results in a slow convergence. Its value should be chosen sufficiently small to enable convergence towards the minimum of the objective function F^h and to preclude chattering. The normalization gain $\eta_{\mathbf{u}}^h$ limits the maximal convergence convergence rate of the optimizer. By normalizing the optimizer gain, we obtain that $\|\Delta\hat{\mathbf{u}}_k^h\| \leq \eta_{\mathbf{u}}$ such that $\frac{\Delta\hat{\mathbf{u}}_k^h}{\alpha_{\boldsymbol{\omega}}^h}$ is uniformly bounded with a bound that is independent of $\alpha_{\boldsymbol{\omega}}^h$ for any value of $\eta_{\mathbf{u}}$ that is proportional to $\alpha_{\boldsymbol{\omega}}^h$.

A. Tuning of the controller

As mentioned, the values of $\alpha_{\boldsymbol{\omega}}^h$ and σ_r should be sufficiently small for a successful controller implementation. The remaining tuning parameters of the controller are chosen such that the resulting closed-loop system exhibits the following time scales, similar to [20] and also [23], [24]:

- fast – active power filter, power grid;
- medium fast – perturbation of the controller;
- medium slow – observer of the controller;
- slow – optimizer of the controller.

This can be achieved by choosing the tuning parameters such that $\frac{1}{N_{\boldsymbol{\omega}}}$, $-\ln(\lambda_{\mathbf{m}}^h) N_{\boldsymbol{\omega}}^h$, $-\frac{\lambda_{\mathbf{u}}^h \alpha_{\boldsymbol{\omega}}^h}{\ln(\lambda_{\mathbf{m}}^h)}$ and $-\frac{\eta_{\mathbf{u}}^h}{\alpha_{\boldsymbol{\omega}}^h \ln(\lambda_{\mathbf{m}}^h)}$ are sufficiently small; see also [29]. As mentioned, the active power filter and the power grid are faster than the controller to ensure that the model in (20) is accurate. The perturbations of the controller are faster than the observer of the controller so that the time window of the observer is sufficiently long for estimating the state vector $\hat{\mathbf{m}}_k^h$ by observing the perturbations in the time signal of y_k^h. Finally, the observer of the controller is faster than the optimizer of the controller to provide an accurate state estimate without much lag. More details about the stability and tuning of the controller can be found in [29].

IV. Case Study: Three-Bus Electrical Grid with Distributed Generators

We consider the three-bus electrical grid with distributed generators in Fig. 2. The electrical grid portrays a simplified shipboard power system. It consists of two generators, three buses with propulsion loads, an active power filter, an LCL filter and RC shunts. The loads are modeled as variable-speed drives with 12-pulse rectifiers. Due to the 12-pulse rectifiers, the dominating harmonics are of the orders $12r \pm 1$ for positive integer values of r. The parameters of the model are presented in Table I. The per-unit model is given relative to the generator power rating. The current that can be produced by the active filter is limited. To avoid unwanted effects due to saturation of the filter current (that is, current clipping), the current

TABLE I
PARAMETERS OF THE ELECTRICAL GRID (WITH $\omega_f = \frac{2\pi}{T_f}$)

Parameter	Value	Unit
Nominal voltage	690	V
Fundamental frequency $\left(\frac{1}{T_f}\right)$	50	Hz
Generator power rating	1	MVA
L_{G1}, L_{G2}	0.2	pu
R_{G1}	$0.1 \cdot L_{G1} \cdot \omega_f$	pu
R_{G2}	$0.1 \cdot L_{G2} \cdot \omega_f$	pu
L_{M1}	0.04	pu
R_{M1}	$0.1 \cdot L_{M1} \cdot \omega_f$	pu
L_{M2}	0.08	pu
R_{M2}	$0.1 \cdot L_{M2} \cdot \omega_f$	pu
C_{S1}, C_{S2}	2	μF
R_{S1}, R_{S2}	2	Ω
L_{L1}, L_{L2}	0.3	mH
R_{L1}, R_{L2}	0.03	Ω
C_C	30	μF
R_C	10	Ω
R_D	160	Ω

references given to the active power filter are cut off if they exceed the maximal current that the active power filter control can produce. Because the models of the grid and the active power filter are similar to the ones used in [17], the reader is kindly referred to [17] for more information. The simulations in this section are conducted in MATLAB/Simulink using the Simscape Power Systems toolbox.

We use the extremum-seeking control method in Section III to compute the optimal parameters u_1^h and u_2^h of the current reference (3) of the active power filter for the harmonics $h \in \{11, 13, 23, 25\}$. The sampling time of the extremum-seeking controller is given by $T_s = 10^{-3}$ s. The tuning parameters are set to $\alpha_{\boldsymbol{\omega}}^{11} = \alpha_{\boldsymbol{\omega}}^{13} = 0.02$ pu, $\alpha_{\boldsymbol{\omega}}^{23} = \alpha_{\boldsymbol{\omega}}^{25} = 0.01$ pu, $N_{\boldsymbol{\omega}}^h = 80$, $\lambda_{\mathbf{m}}^h = 0.887$, $\lambda_{\mathbf{u}}^{11} = \lambda_{\mathbf{u}}^{13} = 8$ pu, $\lambda_{\mathbf{u}}^{23} = \lambda_{\mathbf{u}}^{25} = 4$ pu, $\eta_{\mathbf{u}}^{11} = \eta_{\mathbf{u}}^{13} = 4 \times 10^{-3}$, $\eta_{\mathbf{u}}^{23} = \eta_{\mathbf{u}}^{25} = 10^{-3}$ and $\sigma_r^h = 10^{-3}$ for all $h \in \{11, 13, 23, 25\}$. The applied cost function in (12) is $J^h = \sum_{j=1}^{3} \left((A_{j,a}^h)^2 + (A_{j,b}^h)^2 + (A_{j,c}^h)^2 \right)$, where $A_{j,a}^h$ is the amplitude of the hth harmonic of the voltage in bus j that is obtained from the fast Fourier transform of the voltage signal of phase a. The amplitudes $A_{j,b}^h$ and $A_{j,c}^h$ are defined similarly such that $J^h = 3 \sum_{j=1}^{3} (A_j^h)^2$ if $A_j^h = A_{j,a}^h = A_{j,b}^h = A_{j,c}^h$ under steady-state balanced conditions. It is essential that the perturbation amplitude is sufficiently large so that the effect of the perturbations can be observed in the voltage amplitude signals in order to estimate the gradient of the objective function; see Section III. However, because the resulting oscillations in the voltage amplitude signals impair the obtained steady-state performance, the perturbation amplitude is chosen to be relatively small. To illustrate the difference between local and system-wide harmonic mitigation, we compare our results with those of a local-filtering method. The local-filtering method extracts the 11th, 13th, 23rd and 25th harmonic from current measurements of the local load (Load 2) using a fast Fourier transform and provides the same harmonics with an opposite phase to the active power filter as current reference, similar to [31]. The extremum-seeking control method can easily be combined with other methods. To demonstrate this, we additionally present results for a combination of the extremum-seeking method and the local-filtering method. For this combined method, the current reference that is supplied to the active power filter is the sum of the current references of the extremum-seeking control method and the local-filtering method. The current reference of the local-filtering method acts as a "feedforward" to the extremum-seeking controller in order to respond faster to changing grid conditions. Moreover, we also compare our results with those of the model-predictive control method in [14]–[18]. The model-predictive control method uses a simplified two-bus grid model, where Load 2 and Load 3 are replaced by a single load with an equivalent combined power. The two-bus model has fewer states and parameters than a three-bus model, which makes model identification easier and the computational burden lower. However, because Bus 3 is not contained in the simplified model of the model-predictive controller, the resulting current injection of the active power filter only targets the harmonic distortion in Bus 1 and Bus 2. Because modeling and monitoring all loads that are connected to and disconnected from the electrical grid of a ship is often practically infeasible, it is commonly necessary to resort to model simplifications similar to the one here.

A. Constant load conditions

We use the total harmonic distortion (THD) as a measure for the mitigation performance, where the total harmonic distortion of the voltage in Bus j, with $j \in \{1, 2, 3\}$, is given by

$$\text{THD}_j = \frac{\sqrt{(V_{rms,j}^2)^2 + (V_{rms,j}^3)^2 + (V_{rms,j}^4)^2 + \dots}}{V_{rms,j}^1}, \quad (29)$$

where $V_{rms,j}^h$ is the root-mean-square value of the hth voltage harmonic in Bus j. Table II present the total harmonic distortion of the voltage in the buses under different constant load conditions, where the power of Load 1, Load 2 and Load 3 is denoted by P_1, P_2 and P_3, respectively. From Table II, we obtain the total harmonic distortion of the model-predictive control (MPC) method and the extremum-seeking control (ESC) method are comparable for low-load conditions. For high-load conditions, the electrical grid is more sensitive to the applied harmonic compensation. Because the model imperfections are more predominant under high-load conditions, the model-predictive controller performs slightly worse than the extremum-seeking controller under these conditions. Because the model-predictive controller is designed to mitigate the harmonic distortion in Bus 1 and Bus 2 only, the harmonic distortion in Bus 3 may be much larger than the distortion in the other two buses under certain load conditions, as shown in Table II. The extremum-seeking control method, on the other hand, uses voltage measurements from all three buses and is therefore able to mitigate the distortion in the buses

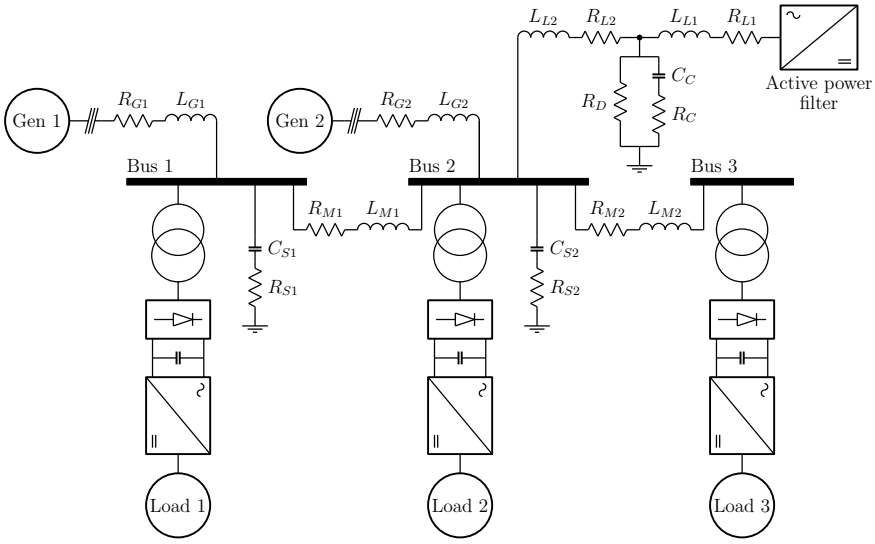

Fig. 2. Model of three-bus shipboard power system.

more evenly. Compared to these two system-wide harmonic-mitigation methods, the local-filtering method (Local) performs significantly worse. Combining the extremum-seeking control method and the local-filtering method (Local + ESC) gives a performance that is similar to that of the extremum-seeking control method. The amount of harmonic distortion of the voltages in the buses mildly oscillates if the extremum-seeking controller is applied due to the use of perturbations; see Section III. To obtain the constant THD values in Table II, the root-mean-square values of the corresponding voltage harmonics are computed by taking the mean over a sufficiently long time interval.

B. Dynamic load conditions

To compute the total harmonic distortion under dynamic load conditions, the length of the time window for the THD calculation is set to the wavelength of the fundamental frequency. In Fig. 3, the THD dynamic responses to a step in the power of the loads are displayed; the power of Load 1 and Load 2 is increased from 0.3 pu to 1.0 pu at time zero, while the power of Load 3 is kept constant at zero. The oscillations in the voltage THD signals of the extremum-seeking control method are due to the used perturbations. Due to the increased sensitivity of electrical grid to the applied harmonic mitigation for high-load conditions, the amplitude of the oscillations is larger for high-load conditions than for low-load conditions. Compared to the model-predictive control method and the local-filtering method, it takes the extremum-seeking control method longer to adapt to the new power levels of the loads. The convergence is faster for the combined extremum-seeking control and local-filtering method, but not as fast as for the model-predictive control or the local-filtering methods.

To simulate the shipboard system during dynamic-positioning operation under rough sea conditions, we apply a sinusoidal oscillation to the power of Load 1 and Load 2 while the power of Load 3 is kept at zero. The power of Load 1 and Load 2 oscillates between 0.3 pu and 1.0 pu with a wavelength of five seconds. The voltage THD signals in the buses during one oscillation are presented in Fig.4. Similar to Fig. 3, the THD values and the magnitude of the perturbation-related oscillations correlate to the load power. Although the response of the extremum-seeking controller is too slow to effectively mitigate the harmonic distortion around times 0.5 s and 3 s, the combined extremum-seeking control and local-filtering method is able to better track the load changes due to a higher convergence rate, which leads to a lower THD around these times. We note that the convergence rate and

TABLE II
PERCENTAGE OF TIME-AVERAGED VOLTAGE THD IN THE BUSES FOR CONSTANT LOAD CONDITIONS IN pu

	MPC	Local	ESC	Local + ESC	P_1	P_2	P_3
THD_1 [%]	5.17	6.44	3.84	3.85			
THD_2 [%]	4.88	5.58	3.65	3.67	1	1	0
THD_3 [%]	4.86	5.59	3.65	3.66			
THD_1 [%]	1.82	3.03	2.03	2.04			
THD_2 [%]	2.04	2.63	1.94	1.97	0.3	0.3	0
THD_3 [%]	2.04	2.57	1.94	1.97			
THD_1 [%]	2.52	6.08	2.88	2.89			
THD_2 [%]	2.50	5.12	2.20	2.22	1	0.3	0
THD_3 [%]	2.49	5.13	2.20	2.22			
THD_1 [%]	2.07	3.92	2.25	2.26			
THD_2 [%]	2.36	3.96	2.33	2.33	0.3	1	0
THD_3 [%]	2.36	3.94	2.33	2.33			
THD_1 [%]	3.93	5.70	3.08	3.10			
THD_2 [%]	2.91	5.35	2.57	2.59	1	1	1
THD_3 [%]	5.65	8.24	4.10	4.11			
THD_1 [%]	1.66	3.26	2.37	2.38			
THD_2 [%]	1.90	3.96	2.22	2.23	0.3	0.3	1
THD_3 [%]	5.18	7.62	4.31	4.31			

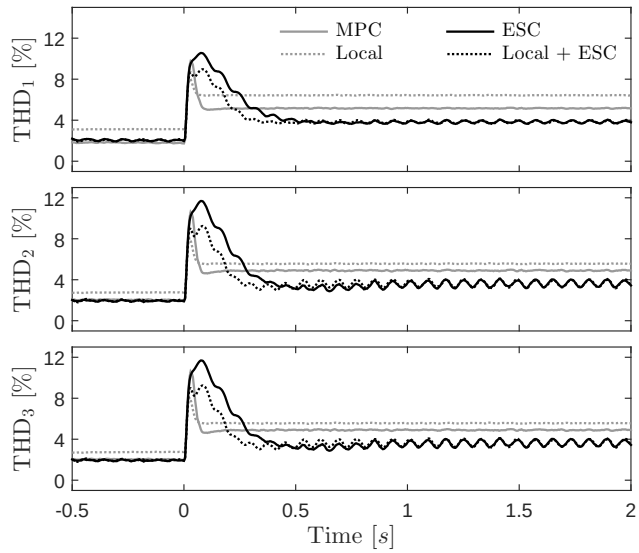

Fig. 3. Percentage of voltage THD in the buses as a function of time as the values of P_1 and P_2 jump from 0.3 pu to 1.0 pu at time zero while P_3 remains zero.

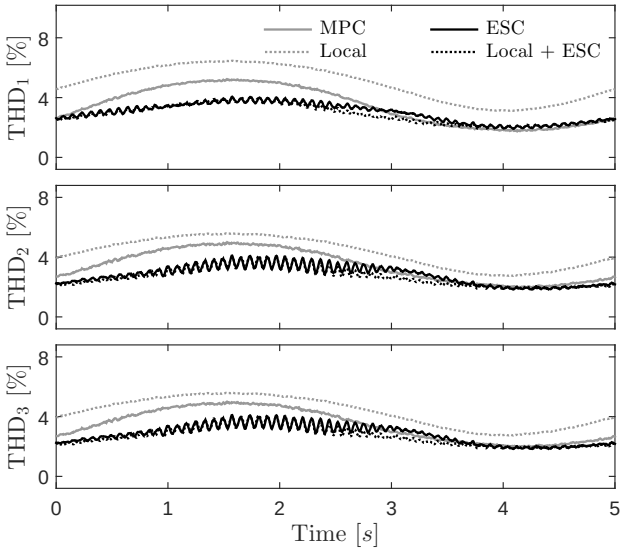

Fig. 4. Percentage of voltage THD in the buses as a function of time as the values of P_1 and P_2 oscillate between 0.3 pu and 1.0 pu with a wavelength of five seconds while P_3 remains zero.

the steady-state performance (including the amplitude of the oscillations due to the perturbations) of the extremum-seeking control method and the combined method depend on the tuning of the extremum-seeking controllers. A faster convergence will generally deteriorate the steady-state performance due to the tuning trade-off discussed in [24].

V. Conclusion

In this work, we have presented an extremum-seeking control method that optimizes the injection current of an active power filter for the system-wide minimization of harmonic distortion in electrical grids of marine vessels. The main advantage of the presented method compared to alternative methods is that no grid model is required. The presented method is computationally cheap compared to model-based system-wide harmonic mitigation methods, can easily be applied to an electrical grid with an arbitrary number of nodes, and can be implemented on top of existing methods. A case study of a three-bus electrical grid displays that an equally good or superior steady-state harmonic mitigation can be achieved with the presented method compared to a model-predictive control method and a local-filtering method. The convergence rate of the extremum-seeking control method is lower, but can be improved by combining the extremum-seeking control method and the local-filtering method without significant loss of steady-state performance.

References

[1] K. B. Ariyur and M. Krstić, *Real-time optimization by extremum-seeking control*. Hoboken, NJ: Wiley-Interscience, 2003.

[2] Y. Tan, W. H. Moase, C. Manzie, D. Nešić, and I. M. Y. Mareels, "Extremum seeking from 1922 to 2010," in *Proceedings of the 29th Chinese Control Conference*, pp. 14–26, Beijing, China, July 29-31, 2010.

[3] J. Mindykowski, "Case study-based overview of some contemporary challenges to power quality in ship systems," *Inventions*, vol. 1, no. 2, 12 2016.

[4] S. G. Jayasinghe, L. Meegahapola, N. Fernando, J. Z., and J. M. Guerrero, "Review of ship microgrids: system architectures, storage technologies and power quality aspects," *Inventions*, vol. 2, no. 1, 4 2017.

[5] T. Key and J.-S. Lai, "Analysis of harmonic mitigation methods for building wiring systems," *IEEE Transactions on Power Systems*, vol. 13, no. 3, pp. 890–897, 1998.

[6] G. K. Singh, "Power system harmonics research: a survey," *European Transactions on Electrical Power*, vol. 19, no. 2, pp. 151–172, 2009.

[7] H. Akagi, E. H. Watanabe, and M. Aredes, *Instantaneous power theory and applications to power conditioning*. Hoboken, New Jersey: John Wiley & Sons, 2007.

[8] M. El-Habrouk, M. K. Darwish, and P. Mehta, "Active power filters: a review," *IEE Proceedings - Electric Power Applications*, vol. 147, no. 5, pp. 403–413, 2000.

[9] W. M. Grady, M. J. Samotyj, and A. H. Noyola, "Survey of active power line conditioning methodologies," *IEEE Transactions on Power Delivery*, vol. 5, no. 3, pp. 1536–1542, 1990.

[10] B. Singh, K. Al-Haddad, and A. Chandra, "A review of active filters for power quality improvement," *IEEE Transactions on Industrial Electronics*, vol. 46, no. 5, pp. 960–971, 1999.

[11] K. Wada, H. Fujita, and H. Akagi, "Considerations of a shunt active filter based on voltage detection for installation on a long distribution feeder," *IEEE Transactions on Industry Applications*, vol. 34, no. 4, pp. 1123–1130, 2002.

[12] W. M. Grady, M. J. Samotyj, and A. H. Noyola, "Minimizing network harmonic voltage distortion with an active power line conditioner," *IEEE Transactions on Power Delivery*, vol. 6, no. 4, pp. 1690–1697, 1991.

[13] W. M. Grady, M. J. Samotyj, and A. H. Noyola, "The application of network objective functions for active minimizing the impact of voltage harmonic in power systems," *IEEE Transactions on Power Delivery*, vol. 7, no. 3, pp. 1379–1386, 1992.

[14] E. Skjong, M. Ochoa-Gimenez, M. Molinas, and T. A. Johansen, "Management of harmonic propagation in a marine vessel by use of optimization," in *IEEE Transportation Electrification Conference and Expo (ITEC)*, pp. 1–8, 2015.

[15] E. Skjong, M. Molinas, and T. A. Johansen, "Optimized current reference generation for system-level harmonic mitigation in a diesel-electric ship using non-linear model predictive control," in *IEEE International Conference on Industrial Technology (ICIT)*, pp. 2314–2321, 2015.

[16] E. Skjong, M. Molinas, T. A. Johansen, and R. Volden, "Shaping the current waveform of an active filter for optimized system level harmonic conditioning," in *Proceedings of the 1st International Conference on Vehicle Technology and Intelligent Transport Systems*, pp. 98–106, 2015.

[17] E. Skjong, J. A. Suul, A. Rygg, M. Molinas, and T. A. Johansen, "System-wide harmonic mitigation in a diesel electric ship by model predictive control," *IEEE Transactions on Industrial Electronics*, vol. 63, no. 7, pp. 4008–4019, 2016.

[18] E. Skjong, J. A. Suul, M. Molinas, and T. A. Johansen, "Optimal compensation of harmonic propagation in a multi-bus microgrid," *Renewable Energy and Power Quality Journal*, vol. 14, pp. 236–241, 2016.
[19] M. Guay and D. Dochain, "A time-varying extremum-seeking control approach," *Automatica*, vol. 51, pp. 356–363, 2015.
[20] M. Haring and T. A. Johansen, "Asymptotic stability of perturbation-based extremum-seeking control for nonlinear plants," *IEEE Transactions on Automatic Control*, vol. 62, no. 5, pp. 2302–2317, 2017.
[21] J. Mindykowski and T. Tarasiuk, "Problems of power quality in the wake of ship technology development," *Ocean Engineering*, vol. 107, pp. 108–117, 2015.
[22] T. Tarasiuk, "Comparative study of various methods of DFT calculation in the wake of IEC standard 61000-4-7," *IEEE Transactions on Instrumentation and Measurement*, vol. 58, no. 10, pp. 3666–3677, 2009.
[23] M. Krstić and H.-H. Wang, "Stability of extremum seeking feedback for general nonlinear dynamic systems," *Automatica*, vol. 36, no. 4, pp. 595–601, 2000.
[24] Y. Tan, D. Nešić, and I. M. Y. Mareels, "On non-local stability properties of extremum seeking control," *Automatica*, vol. 42, no. 6, pp. 889–903, 2006.
[25] H. Yu and U. Ozguner, "Extremum-seeking control strategy for ABS system with time delay," in *Proceedings of the American Control Conference*, Anchorage, AK, May 8-10, 2002.
[26] M. Haring, N. van de Wouw, and D. Nešić, "Extremum-seeking control for nonlinear systems with periodic steady-state outputs," *Automatica*, vol. 49, no. 6, pp. 1883–1891, 2013.
[27] M. Krstić, "Performance improvement and limitations in extremum seeking control," *Systems & Control Letters*, vol. 39, no. 5, pp. 313–326, 2000.
[28] W. H. Moase and C. Manzie, "Semi-global stability analysis of observer-based extremum-seeking for Hammerstein plants," *IEEE Transactions on Automatic Control*, vol. 57, no. 7, pp. 1685–1695, 2012.
[29] M. A. M. Haring, "Extremum-seeking control: convergence improvements and asymptotic stability," Ph.D. dissertation, Norwegian University of Science and Technology, 2016.
[30] R. M. Johnstone and B. D. O. Anderson, "Exponential convergence of recursive least squares with exponential forgetting factor," *Systems & Control Letters*, vol. 2, no. 2, 1982.
[31] S. M. Williams and R. G. Hoft, "Adaptive frequency domain control of PWM switched power line conditioner," *IEEE Transactions on Power Electronics*, vol. 6, no. 4, pp. 665–670, 1991.

Mark Haring received his BSc degree and MSc degree in mechanical engineering from Eindhoven University of Technology, Eindhoven, The Netherlands, in 2008 and 2011, respectively. In 2016, he obtained his PhD degree in engineering cybernetics at NTNU, the Norwegian University of Science and Technology, Trondheim, Norway.

He is currently working as a postdoctoral researcher at the Department of Engineering Cybernetics, NTNU. His research interests include automatic control, adaptive control, and estimation.

Espen Skjong received his MSc and PhD degree in Engineering Cybernetics at the Norwegian University of Science and Technology (NTNU), Trondheim, Norway, in 2014 and 2017, respectively. During his PhD he specialized in optimal control of shipboard electrical systems, and the control of active filters to obtain optimal system-level harmonic mitigation in AC grids using Model Predictive Control (MPC). During his MSc he specialized in MPCs for autonomous control of Unmanned Aerial Vehicles (UAVs).

He is currently employed in Ulstein Blue Ctrl AS (Ålesund, Norway) as Research, Development and Technology (RD&T) Manager. His main research interest is centered around optimal control and control applications for marine vehicles.

Tor Arne Johansen (M'98, SM'01) received the MSc degree in 1989 and the PhD degree in 1994, both in electrical and computer engineering, from the Norwegian University of Science and Technology (NTNU), Trondheim, Norway.

From 1995 to 1997, he worked at SINTEF as a researcher before he was appointed Associated Professor at NTNU in Trondheim in 1997 and Professor in 2001. He has published several hundred articles in the areas of control, estimation and optimization with applications in the marine, automotive, biomedical and process industries. In 2002, he co-founded the company Marine Cybernetics AS where he was Vice President until 2008.

Prof. Johansen received the 2006 Arch T. Colwell Merit Award of the SAE, and is currently a principal researcher within the Center of Excellence on Autonomous Marine Operations and Systems (AMOS) and director of the Unmanned Aerial Vehicle Laboratory at NTNU.

Marta Molinas (M'94) received the Diploma degree in electromechanical engineering from the National University of Asuncion, Asuncion, Paraguay, in 1992; the Master of Engineering degree from Ryukyu University, Japan, in 1997; and the Doctor of Engineering degree from the Tokyo Institute of Technology, Tokyo, Japan, in 2000.

She was a Guest Researcher with the University of Padova, Padova, Italy, during 1998. From 2004 to 2007, she was a Postdoctoral Researcher with the Norwegian University of Science and Technology (NTNU) and from 2008-2014 she has been professor at the Department of Electric Power Engineering at the same university. From 2008 to 2009, she was a Japan Society for the Promotion of Science (JSPS) Research Fellow with the Energy Technology Research Institute, National Institute of Advanced Industrial Science and Technology, Tsukuba, Japan. In 2014, she was Visiting Professor at Columbia University and Invited Fellow by the Kingdom of Bhutan working with renewable energy microgrids for developing regions. She is currently Professor at the Department of Engineering Cybernetics, NTNU. Her research interests include stability of power electronics systems, harmonics, oscillatory phenomena, and non-stationary signals from the human and the machine.

Dr. Molinas has been an AdCom Member of the IEEE Power Electronics Society. She is Associate Editor and Reviewer for *IEEE Transactions on Power Electronics* and *PELS Letters*.